BIFURCATION OF PLANETARY BUILDING BLOCKS DURING SOLAR SYSTEM FORMATION. T. Lichtenberg[1], J. Drążkowska[2], M. Schönbächler[3], G. J. Golabek[4], T. O. Hands[5], [1]Atmospheric, Oceanic and Planetary Physics, Department of Physics, University of Oxford, UK, [2]University Observatory, Faculty of Physics, Ludwig-Maximilians-Universität München, Germany, [3]Institute for Geochemistry and Petrology, Department of Earth Sciences, ETH Zurich, Switzerland (mariasc@ethz.ch), [4]Bayerisches Geoinstitut, University of Bayreuth, Germany, [5]Institute for Computational Science, University of Zurich, Switzerland.

Introduction: Geochemical and astronomical evidence demonstrates that planet formation occurred in two spatially and temporally separated reservoirs. The origin of this dichotomy is unknown. We use numerical models to investigate how the evolution of the solar protoplanetary disk influenced the timing of protoplanet formation and their internal evolution [1]. Migration of the water snow line can generate two distinct bursts of planetesimal formation that sample different source regions. These reservoirs evolve in divergent geophysical modes and develop distinct volatile contents. This is consistent with constraints from meteorites on the accretion chronology, thermochemistry, and the significantly smaller mass locked in planetary bodies of the inner Solar System compared to the outer part. Our simulations suggest that the compositional fractionation and isotopic dichotomy of the inner and outer Solar System was initiated by the interplay between disk dynamics, heterogeneous accretion, and internal evolution of forming protoplanets.

Fragmented Accretion of Solar System(s): Astronomical surveys of planet-forming circumstellar disks identify substructures and rapid dust coagulation within the disk [2]. The observations indicate that the total dust mass in observable dust grains decreases rapidly with disk age. This suggests that the initial steps of planet formation start early in the Class I disk stage, when the protoplanetary disk is built-up from the surrounding molecular cloud. Indications for grain growth and substructure in this stage [3] corroborate geochemical evidence from Solar System materials that provide evidence for spatial substructure during early planet formation. This is for example recorded in the dichotomy of supernovae-derived isotopes between the inner and outer solar system i.e., the non-carbonaceous (NC) and carbonaceous (CC) reservoirs [4,5]. The timing and spatial separation of these two reservoirs based on evidence from the meteorite record contains information about the chronology of the planet formation process [6,7] and the relation between the volatile-depleted inner and volatile-rich outer Solar System. However, the physical processes that inflicted the observed signatures are debated in the community [8,9].

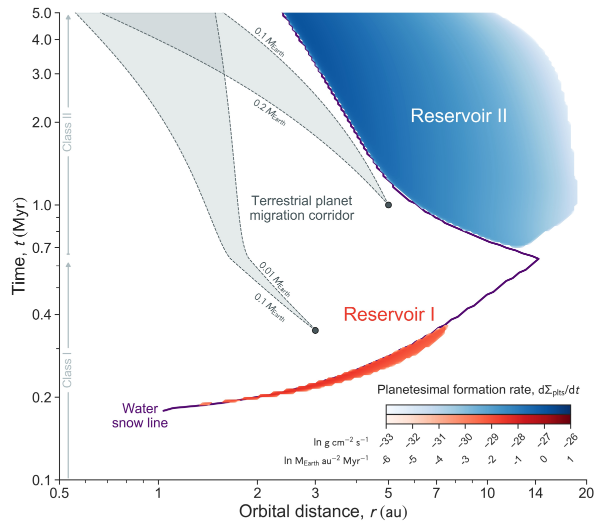

***Fig. 1**: Formation of two distinct planetesimal populations in the disk simulation. The disk is built-up during the Class I (infall) stage. During this time, the disk heats up and the snow line (purple) moves outward. Once infall stops, the disk cools, and the snow line moves inward. Two distinct populations of planetesimals (red and blue areas) form at the location of the snow line due to condensation and sublimation effects of the drifting ice-dust grains (pebbles). The dashed gray lines define the range of possible planet migration scenarios consistent with the present-day orbits of the terrestrial planets.*

Two Planetesimal Formation Bursts: In order to connect the geochemical to astronomical evidence, we use numerical models to show that midplane-quiescent protoplanetary disks can form two distinct bursts of planetesimal formation in the inner and outer disk [10] (*Fig. 1*). The two bursts are formed due to the movement of the water snow line during the Class I and Class II disk phase in interaction with the drifting dust grains, which trigger the formation of an early planetesimal population in the inner disk (Reservoir I), and a later population in the outer disk (Reservoir II) in the Class II stage.

The two reservoirs deviate in their total generated planetesimal mass by more than an order of magnitude and form over two distinct time intervals at different orbits. Reservoir II develops over an extended time interval, starting from about 0.7 Myr after calcium-aluminum-rich inclusions (CAI) formation until disk gas dissipation. During this time, the inner disk becomes substantially depleted in pebbles because pebbles from the outer disk are mainly incorporated into the outer planetesimal population. The local pebble flux to the inner Reservoir I is more than one order of magnitude lower compared to the outer one. This substantially limits mixing between the two reservoirs by inward dust drift. Therefore, it can explain the extended time both reservoirs were separated as evidenced by nucleosynthetic isotope compositions (dichotomy) and dating of meteorites.

Divergent Evolution of Protoplanets in Inner and Outer Solar System: The two planetesimal populations differ substantially in formation time and thus internal radiogenic heating from ^{26}Al. We performed numerical simulations of the two planetesimal populations [11], and tested whether their internal thermochemical evolution aligns with the chronology of metal-silicate segregation and aqueous alteration recorded in meteorites. We find that the difference in formation times of Reservoir I and II leads to substantial differences in geophysical and geochemical evolution of the two birth planetesimal populations. The models reproduce the clustering of core segregation ages in both NC and CC meteorites (*Fig. 2*), the timing of aqueous alteration in CC bodies, and the volatile depletion of the inner compared to the outer Solar System through planetary degassing.

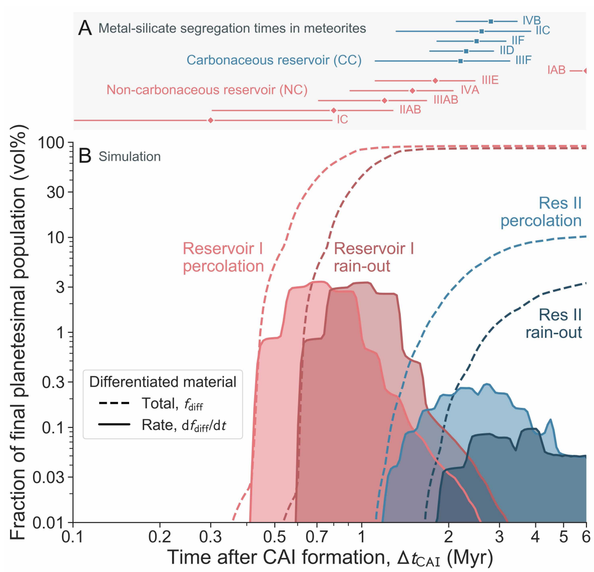

Fig. 3: Comparison of metal-silicate separation times in simulated planetesimal populations with the meteorite record. (A) Metal-silicate separation times in NC and CC meteorite classes. (B) Timing of core formation in Reservoir I (red) or Reservoir II (blue). Solid lines with colored shading represent the fraction of material undergoing metal-silicate separation. Dashed lines show the total volumetric fraction for each scenario over time. Light and dark red/blue indicate iron core formation by percolation or metal rain-out in planetesimal magma oceans, respectively.

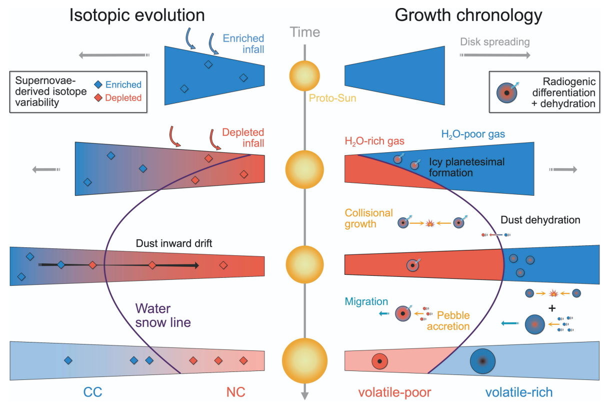

Fig. 2*: Schematic illustration of early planetary accretion. The nucleosynthetic isotope dichotomy (left) across the disk is built up due to varying compositions of infall material. It is retained by the pile-up of inward-drifting dust at the snow line. The formation of two distinct planetesimal populations initiates divergent evolutionary pathways of inner and outer Solar System (right) due to the secular variation of local material composition, internal radiogenic heating, and dominant mode of planetary growth.*

Our modelling suggests that the terrestrial protoplanets underwent a secular change in growth mode from early collisions to pebble accretion to a final pebble-starved (collisional) phase before cessation of the gas disk. It can account for seemingly opposing accretion chronologies as inferred from Hf-W [12] and Ca [13] isotope systems, the fractionation in mass-dependent isotopes of terrestrial planetary bodies [14,15], and the absence of super-Earths in the inner Solar System.

Accretion Framework for Planet Formation: Based on our simulations we propose a new accretion framework for the early Solar System [1] (*Fig. 3*) that can reconcile characteristics from geochemical chronology with the structure, time evolution, and dust mass depletion in astrophysical disks. It offers testable hypotheses to further refine the earliest formation environment of planet formation in the Solar System.

References: [1] Lichtenberg T. et al. (2021) *Science, 371*, 6527. [2] Andrews S. M. (2020) *Annu. Rev. Astron. Astrophys., 58*, 483–528. [3] Segura-Cox et al. (2020) *Nature, 586*, 228. [4] Leya I. et al. (2008) *E&PSL, 266*, 233. [5] Warren, P. H. (2011) *E&PSL, 311*, 93. [6] Desch S. J. et al. (2018) *ApJS, 238*, 11. [7] Alibert, Y. et al. (2018) *Nat. Astron., 2*, 873–877. [8] Mezger K. et al. (2020) *Space Sci. Rev., 216*, 27. [9] Kruijer T. S. et al. (2019) *Nat. Astron., 4*, 32–40. [10] Drążkowska J. & Dullemond C. P. (2018) *A&A, 614*, A62. [11] Lichtenberg T. et al. (2019) *Nat. Astron., 3*, 307. [12] Nimmo F. et al. (2018) *Space Sci. Rev., 214*, 101. [13] Schiller M. et al. (2018) *Nature, 555*, 507–510. [14] Hin R. C. et al. (2017) *Nature, 549*, 511–515. [15] Norris & Wood (2017) *Nature, 549*, 507–510.